Ionic Selectivity, Saturation, and Block in Sodium Channels

A Four-Barrier Model

BERTIL HILLE

From the Department of Physiology and Biophysics, University of Washington School of Medicine, Seattle, Washington 98195

ABSTRACT Ionic fluxes in Na channels of myelinated axons show ionic competition, block, and deviations from simple flux independence. These phenomena are particularly evident when external Na^+ ions are replaced by other permeant or impermeant ions. The observed currents require new flux equations not based on the concepts of free diffusion. A specific permeability model for the Na channel is developed from Eyring rate theory applied to a chain of saturable binding sites. There are four energy barriers in the pore and only one ion is allowed inside at a time. Deviations from independence arise from saturation. The model shows that ionic permeability ratios measured from zero-current potentials can differ from those measured from relative current amplitudes or conductances. The model can be fitted to experiments with various external sodium substitutes by varying only two parameters: For each ion the height of the major energy barrier (the selectivity filter) determines the biionic zero-current potential and the depth of the energy well (binding site) just external to that barrier then determines the current amplitudes. Voltage clamp measurements with myelinated nerve fibers are given showing numerous examples of deviations from independence in ionic fluxes. Strong blocks of ionic currents by guanidinium compounds and Tl^+ ions are fitted by binding within the channel with apparent dissociation constants in the range 50–122 mM. A small block with high Na^+ concentrations can be fitted by Na^+ ion binding with a dissociation constant of 368 mM. The barrier model is given a molecular interpretation that includes stepwise dehydration of the permeating ion as it interacts with an ionized carboxylic acid.

Ionic channels in nerve and muscle membranes gate the flow of metal cations to make the membrane electrically excitable (Hodgkin and Huxley, 1952 *c*). Several features of the ionic fluxes have properties like aqueous diffusion. Individual permeant ions move in both directions through open channels, driven by thermal agitation and by electric fields in the membrane. For any

given ionic concentrations and membrane potential, the net flux of ions is in the direction that tends to reduce ionic electrochemical activity differences across the membrane. Also the temperature coefficients of fluxes in open channels are low (Q_{10} = 1.3–1.5) indicating that the enthalpy barriers to flow are about as low as in ordinary aqueous diffusion. For these and other reasons neurophysiologists usually discuss ion flow in channels using integrated equations of electrodiffusion derived from the differential Nernst-Planck equations for free diffusion of ions in a viscous medium.

By far the most useful and important of the integrated electrodiffusion equations in electrophysiology are the Goldman (1943), Hodgkin and Katz (1949) current and voltage equations. These equations are mainstays of our modern theory relating permeability, concentration, membrane potential, and current. As ordinarily derived, the Goldman-Hodgkin-Katz constant-field theory also contains the assumptions necessary for systems obeying the "independence relation" of Hodgkin and Huxley (1952 *a*) and the Ussing (1949) flux ratio test for free diffusion. In addition, the constant-field theory assumes a homogeneous membrane with a constant diffusion coefficient from one side to another and with identical simple ionic partition coefficients on the two sides. Selectivity arises because the product of the diffusion coefficient times the partition coefficient differs for different ions. In the Goldman-Hodgkin-Katz theory the two factors contributing to selectivity cannot, however, be separated by measurements of current, voltage, and concentration.

This paper presents a different description of ions moving in pores where the partition coefficients and diffusion coefficients are separable. The motivation for developing this theory came from the discovery that currents carried in Na channels by several sodium substitutes like thallous or guanidinium ions are smaller than predicted by the conventional theory, almost as if the substitutes had an anesthetic effect (Hille, 1971, 1972). Evidently ions added to the external solution can compete with other ions or even block their flow in Na channels. However the blocking effect is voltage dependent and may occur within the channels rather than just at the membrane surface.

The experimental literature contains several clear disagreements between observation and the existing electrodiffusion theory. For example, potassium fluxes in *Sepia* giant axons do not fit the Ussing flux ratio (Hodgkin and Keynes, 1955) and instead behave as if ions were moving in single file. In addition the shape of "instantaneous" current-voltage relations of K channels can be changed in a highly voltage-dependent manner by placing various small cations inside axons (Bezanilla and Armstrong, 1972; Hille, 1975 *b*). Similarly the shape of peak current-voltage relations in Na channels can be changed by placing various small cations in the extracellular medium (Hille, 1971, 1972; Woodhull, 1973). Even Na^+ ions appear to block the movement

of other Na^+ ions in the Na channel (Hille, 1975 *b*). In each of these papers it was suggested that the deviations from independence could be attributed to saturable ion binding sites within the channel, an assumption not readily treated by a free diffusion model. It is the purpose of this paper to give a fuller quantitative base to the saturation hypothesis in Na channels and to describe a four-barrier model of the channel that satisfactorily describes ionic selectivity, deviations from independence due to saturation, and voltage-dependent block by ions. The new flux equations are derived from Eyring rate theory (Glasstone et al., 1941) and standard chemical kinetics. Such models are capable of dealing with flux coupling as in single-file diffusion with saturation, and with "diffusion coefficients" (jump rates) and "partition coefficients" (energy valley levels) that vary from point to point in the channel. Most of the results follow from principles already reviewed in detail by Heckmann (1972), by Läuger (1973), and by Hille (1975 *b*). A preliminary account of the model has appeared (Hille, 1975 *a*). A simplified three-barrier version of the model presented in this paper is given in an article by Chizmadjev et al. (1974) and a book by Markin and Chizmadjev (1974).

THEORY

This section describes some general principles in the application of Eyring absolute reaction rate theory to electrodiffusion and gives the specific model chosen to represent the Na channel.

Absolute Reaction Rate Theory

Eyring rate theory (Glasstone et al., 1941; Frost and Pearson, 1961) describes any rate process, from diffusion to chemical reaction, in terms of elementary jumps over energy barriers. Progress over each barrier is proportional to the number of molecules attaining the extra energy needed to form the "activated complex" or "transition state." The rate constant k_i for passing over a barrier is related to the standard Gibbs free energy of activation $\Delta G_i^{\ddagger}$ ("barrier height") by

$$k_i = \kappa_i(kT/h)\exp(-\Delta G_i^{\ddagger}/RT), \qquad (1)$$

where kT/h is $5.80 \times 10^{12}\ s^{-1}$ and RT is 553 cal/mol at 5°C, and κ_i is a "transmission coefficient" nearly always very close to 1.0. Thus diffusion coefficients and partition coefficients of the continuum theory appear in the Eyring rate theory approach simply as a free energy profile representing the membrane by a sequence of energy peaks and valleys. Externally applied electric fields affect the Gibbs free energy of ions within the membrane, so each barrier height ($\Delta G\ddagger$) includes a term due to electrical potential drops between the energy valley and the peak in addition to the "chemical" term. When applied fields are included this way, the rate theory gives solutions to electrodiffusion problems (Zwolinski et al., 1949). In 1949 Eyring et al. derived the flux equation for ions in a nerve membrane represented as a general multibarrier system with a constant electric field. They implicitly assumed inde-

pendence. If the peak amplitude of all barriers is the same and the number of barriers is made large, the flux equation of Eyring et al. (1949) converges to the Goldman-Hodgkin-Katz equation (see Woodbury et al., 1970, and Woodbury, 1971).

An energy profile for the specific barrier model now proposed for the Na channel is given in Fig. 1. There are four barriers for ions to surmount in crossing the membrane from the well-stirred external compartment 1 to the well-stirred internal compartment 5 (equivalent to the axoplasm). The notation selected differs from the conventional Eyring notation, and subscripts have been eliminated for ease in using the same symbols in computer programs. The symbols $G2$, $G23$, etc., stand for the "chemical" component (no external electric field) of the reduced standard Gibbs free energy of an ion in valley 2, at the peak of barrier 23, etc. The reduced free

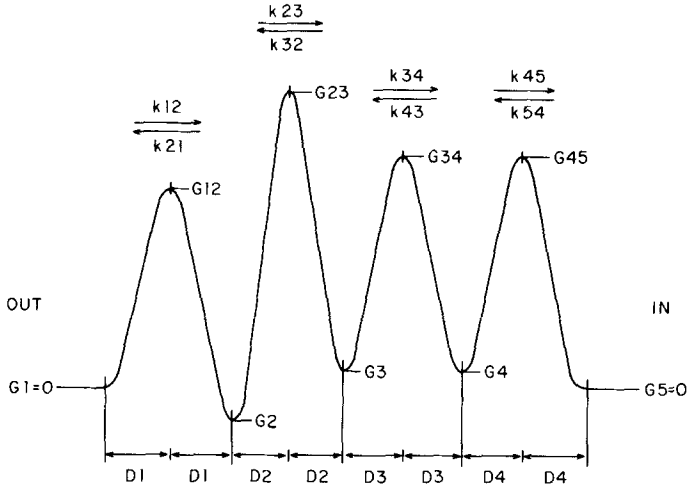

FIGURE 1. A four-barrier energy profile representing the steps of ion movement through the Na channel. The external compartment is 1 and the internal, 5. The rate constants k can be calculated from absolute rate theory knowing the "chemical component" G of the Gibbs free energies at energy peaks and valleys and knowing the fraction D of the total electrical potential drop between a valley and the next peak. The energy levels G and electrical distances D are drawn to scale with the values in Table I.

energy is a dimensionless quantity equal to the conventional free energy divided by RT. If there are several ionic species, e.g., species A and B, their reduced standard free energies are designated $G2$A, $G2$B, etc., and their concentrations in the outer and inner compartments are $C1$A, $C1$B, $C5$A, and $C5$B. More correctly, activities should be used in place of concentrations.

Before the free energy of activation $\Delta G\ddagger$ can be calculated, an electrical component has to be added to the chemical free energies already defined. Electrical potentials are introduced in dimensionless reduced form. The reduced membrane potential V is

$$V = EF/RT,$$

where E is the conventional membrane potential and RT/F is 24.0 mV at 5°C. Quantities $D1$, $D2$, etc., in Fig. 1 define "electrical distances" within the membrane.

They are chosen to be proportional to the fraction of the total membrane potential drop occurring between each energy minimum and the next maximum and scaled to satisfy the condition

$$2 \cdot (D1 + D2 + D3 + D4) = z.$$

The ionic charge z and the factor of 2 are introduced this way to simplify the form of the electrical energy term in the final expression for $\Delta G\ddagger$. It is unnecessary to assume that the electric field is constant across the membrane and therefore the D's need not correspond exactly to linear distance. However from an electrical viewpoint each barrier is assumed to lie half way between neighboring wells. Now the total Gibbs free energy (given the new designation U) at each barrier and valley can be calculated including the effect of the applied field. For example

$$\begin{aligned} U23 &= G23 + V \cdot (2 \cdot D1 + D2) \\ U3 &= G3 + V \cdot (2 \cdot D1 + 2 \cdot D2), \end{aligned}$$

where the second term is the electrical contribution. Finally the conventional simplifying assumption is introduced that all barrier transmission coefficients κ_i are unity (Glasstone et al., 1941; Frost and Pearson, 1961) so the quantity $\kappa_i kT/h$ is replaced by a constant Q. With all these definitions, rate theory (Eq. 1) gives the rate constants of the scheme in Fig. 1, as for example

$$\begin{aligned} k23 &= Q \cdot \exp(-U23 + U2) = Q \cdot \exp(-G23 + G2 - V \cdot D2), \\ k32 &= Q \cdot \exp(-U23 + U3) = Q \cdot \exp(-G23 + G3 + V \cdot D2). \end{aligned}$$

Flux Equations with Barrier Models

Several different flux equations can be derived from the barrier model of Fig. 1 depending on the types of coupling assumed between ions. This section gives equations for a pore without coupling, i.e., obeying the independence relation, and for a saturable pore permitting only one ion to be inside at a time. The approach for a saturable pore accepting several ions moving in single file is also described. The one-ion saturable pore is the model that is used to describe experiments in the Results section.

PORE WITH INDEPENDENCE The system of kinetic equations to solve for ions moving without any mutual interactions is formally the same as that for the linear multicompartment system of Fig. 2 A. The net flux M in the steady state is well known (Eyring et al., 1949; Zwolinski et al., 1949)

$$M = \frac{k12 \left(C5 \dfrac{k21 \cdot k32 \cdot k43 \cdot k54}{k12 \cdot k23 \cdot k34 \cdot k45} - C1 \right)}{1 + \dfrac{k21}{k23} + \dfrac{k21 \cdot k32}{k23 \cdot k34} + \dfrac{k21 \cdot k32 \cdot k43}{k23 \cdot k34 \cdot k45}}. \qquad (2)$$

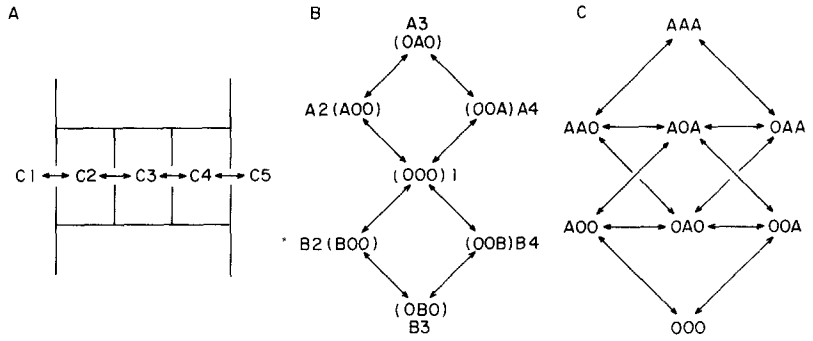

FIGURE 2. Three different kinetic schemes that may be solved in the context of a four-barrier model. (A) A conventional five-compartment scheme with first-order transfer of material between compartments and no restrictions on the internal concentrations *C*1, *C*2, *C*3. This is a finite-difference approximation to conventional electrodiffusion theory, and the solutions for any number of permeant species satisfy independence and Ussing's (1949) flux ratio. (B) A saturating one-ion pore with two permeant species. States of the pore are labeled in two ways, in terms of occupancy (AOO) and by the notation *A*2, etc. used in the computer program. Solutions satisfy Ussing's flux ratio but not independence. (C) A saturating three-ion pore with one permeant species. States of the pore are labeled in terms of occupancy. The ions move in a single-file mechanism based on vacancies rather than on a knock-on process. Solutions do not satisfy independence or Ussing's flux ratio.

In terms of rate theory this simplifies to

$$M = \frac{Q \cdot [C5 \cdot \exp(V) - C1]}{\exp(U12) + \exp(U23) + \exp(U34) + \exp(U45)} . \quad (3)$$

To be strictly correct, the equation should contain ratios of the "thicknesses" or volumes of the compartments as in the cited derivations. The above form is correct if all compartment thicknesses are the same. As a general principle, the depths of internal energy valleys appear in many rate constants but cancel out of the final flux expression for systems satisfying independence (Zwolinski et al., 1949). Depths of energy valleys have *no* influence on fluxes or potentials in systems obeying independence, as can be seen from Eq. 3. When two or more ions are involved, the zero-current potential may be calculated by setting the sum of ionic charge movements equal to zero. The resulting expression is the same as the familiar Goldman-Hodgkin-Katz voltage equation only when, for example, for two ion species A and B with different energy profiles the following condition holds at all potentials:

$$U12A - U12B = U23A - U23B = U34A - U34B = U45A - U45B = \Delta UAB, \quad (4)$$

where ΔUAB is a voltage-independent constant. This condition may be called the "constant offset energy peak condition" (Hille, 1975 *b*) and can be applied to barrier systems with any number of barriers and any number of ions. When Eq. 4 holds, the permeability ratio P_B/P_A is equal to $\exp(\Delta UAB)$.

SATURABLE PORES In this paper saturable pore will mean one in which each internal energy well represents an ion binding site and the number of ions bound

inside is limited. The system of kinetic equations to solve for ions moving in a saturable pore are the same as those for enzyme-substrate reactions or other ordered, sequential binding phenomena. As Heckmann (1968; Heckmann and Vollmerhaus, 1970) has illustrated in solving single-file problems, it is necessary to consider that the channel is constantly making transitions among various "states" of occupancy. These states and the allowed transitions between them must first be written down. If the channel is allowed to contain no more than one ion at a time, then with three internal energy valleys there are only three occupied states (XOO), (OXO), and (OOX) for each permeant ion species and one empty state (OOO). From here on such a channel is called a "one-ion pore." When two permeant ion species A and B are present the one-ion pore has six occupied states and one free state. The eight allowed transitions among these states may be represented by the kinetic diagram in Fig. 2 B. The states are represented in two ways. The notation *A*4, for example, means ion A in site 4 or (OOA). Kinetic solutions of this model are derived later. Many more states must be included if up to three ions are permitted in the pore, one in each energy valley, but ions may not pass each other. Such a channel will be called a "single-file pore." Fig. 2 C is a kinetic diagram of the seven occupied states, one empty state, and twelve transitions needed to describe a single-file pore with three internal energy valleys and only one permeant species A. If permeant ion species B is also present, seven more states with B's and twelve more states with A's and B's mixed are added, and the kinetic scheme becomes impractical to draw. Unlike the one-ion pore, the single-file pore becomes extremely complicated as more permeant species are included.

Kinetic schemes like those of Fig. 2 B or C may be solved by conventional methods to give transient or steady-state solutions. This paper is concerned only with steady-state fluxes. The transient solutions with single-file pores do however have practical interest, for example, in explaining time-courses of block of K channels by internally applied quaternary ammonium ions (Armstrong, 1971). The steady-state solution for any model representable by a diagram ("graph") of states with first-order transitions is conveniently written down without algebraic manipulation by the graph theoretical approach widely used for enzyme reactions (King and Altman, 1956). For large problems a computer algorithm is available to form the terms of the solution (Heckmann et al., 1969). As explained by King and Altman (1956), it is convenient in this approach to redefine those rate constants involving reaction with ions in the external compartments 1 and 5 to include the concentrations $C1$ or $C5$ (or more properly, activities with a standard state of 1 M) as follows:

$$k12 = C1 \cdot Q \cdot \exp(-U12),$$
$$k54 = C5 \cdot Q \cdot \exp(-U45 + U5).$$

This convention is used from now on. The other rate constants involving internal transitions remain as before. With this redefinition, the value of each rate constant corresponds to the maximum rate of transition over each barrier in units of transitions per second, and the final form of the rate equations assumes a simplified form.

Flux equations for one-ion pores of arbitrary length are found in a fairly general form in the treatments of Heckmann et al. (1972) and of Laüger (1973). The main problem is to obtain expressions for the fraction of pores in each allowable state. Fig.

3 gives in the form of a computer program the steady-state solution of the kinetic system of Fig. 2 B, the four-barrier, one-ion pore with two permeant species A and B. Kinetic systems of one-ion pores are exceptionally easy to solve by the King-Altman method (1956) because no matter how many permeant species there are, the solutions for each ion may be developed separately and combined only at the end. In the program of Fig. 3, the 16 rate constants, designated $K12A$, $K21A$, $K12B$, $K21B$,

```
RATE CONSTANTS

    K12A=C1A*EXP(-G12A-V*D1)        K12B=C1B*EXP(-G12B-V*D1)
    K21A=EXP(-G12A+G2A+V*D1)        K21B=EXP(-G12B+G2B+V*D1)
    K23A=EXP(-G23A+G2A-V*D2)        K23B=EXP(-G23B+G2B-V*D2)
    K32A=EXP(-G23A+G3A+V*D2)        K32B=EXP(-G23B+G3B+V*D2)
    K34A=EXP(-G34A+G3A-V*D3)        K34B=EXP(-G34B+G3B-V*D3)
    K43A=EXP(-G34A+G4A+V*D3)        K43B=EXP(-G34B+G4B+V*D3)
    K45A=EXP(-G45A+G4A-V*D4)        K45B=EXP(-G45B+G4B-V*D4)
    K54A=C5A*EXP(-G45A+V*D4)        K54B=C5B*EXP(-G45B+V*D4)

PARTIAL DISTRIBUTION RATIOS

    A1=K32A*K21A*(K43A+K45A)+K34A*K45A*(K21A+K23A)
    A2=K43A*K32A*(K12A+K54A)+K45A*K12A*(K32A+K34A)
    A3=K12A*K23A*(K43A+K45A)+K54A*K43A*(K21A+K23A)
    A4=K23A*K34A*(K12A+K54A)+K21A*K54A*(K32A+K34A)
    B1=K32B*K21B*(K43B+K45B)+K34B*K45B*(K21B+K23B)
    B2=K43B*K32B*(K12B+K54B)+K45B*K12B*(K32B+K34B)
    B3=K12B*K23B*(K43B+K45B)+K54B*K43B*(K21B+K23B)
    B4=K23B*K34B*(K12B+K54B)+K21B*K54B*(K32B+K34B)

MASTER DISTRIBUTION RATIOS

    R1=A1*B1
    R2A=A2*B1                       R2B=B2*A1
    R3A=A3*B1                       R3B=B3*A1
    R4A=A4*B1                       R4B=B4*A1
    RSUM=R1+R2A+R3A+R4A+R2B+R3B+R4B

IONIC FLUXES

    MA=5.8E12*(K21A*R2A-K12A*R1)/RSUM
    MB=5.8E12*(K21B*R2B-K12B*R1)/RSUM
    MNET=MA+MB
```

FIGURE 3. The kinetic equations for the one-ion pore model (Fig. 2 B) with two permeant species A and B, written in the form of a computer program to calculate the partial ionic fluxes MA and MB and the net flux MNET. The first part calculates rate constants from rate theory (Eq. 1) and the remainder is the kinetic solution obtained by the method of King and Altman (1956).

etc., for transitions with the two permeant species are first calculated omitting the constant factor Q. If barrier spacings or ionic valences for the two ions differed it would be necessary here to include different D values for A and B rate constants. The next four lines assemble the four partial distribution ratios formed in the separate King-Altman (1956) solution of the one-ion pore with ion A alone. These quantities are like partition functions for the four states of the pore in the presence of ion A, in that the ratio of the quantities $A1:A2:A3:A4$ is equal to the ratio of the proportion of channels in states 1, 2A, 3A, and 4A in the steady state. The partial distribution ratios for ion B alone are then calculated. Then the master distribution

ratio terms $R1$, $R2A$, $R2B$, etc., and their sum RSUM are calculated by combining the separate solutions. If a third species C were permeant, the distribution ratios would be products of three partial ratios: $A1 \cdot B1 \cdot C1$, $A2 \cdot B1 \cdot C1$, etc. Now the actual fraction of pores in each state is easily calculated. Thus the fraction in state $2B$ is $R2B/R$SUM, and so forth. Finally the net steady-state fluxes MA and MB and the total ionic flux MNET are calculated as the difference of the inward and outward fluxes across one of the barriers (arbitrarily barrier 12). The fluxes are now in absolute terms of ions/(s pore) because the factor Q (5.8×10^{12}) is included. In this paper current-voltage relations are calculated from the equations directly and zero-current potentials are calculated by the Newton-Raphson iterative method, both on a digital computer.

The equations in Fig. 3 for a one-ion pore are those used throughout this paper but it is interesting for future work to comment on solutions of single-file pores (see Heckmann, 1972, for a valuable heuristic discussion). The job in each new case is to write down the distribution ratios R as in Fig. 3. Formally the terms in these ratios are determined only by the topology of the "graph" or diagram of states and connections (Fig. 2 B and C), quite independent of the physical significance of each state or transition. If any of the R's in Fig. 3 for the one-ion pore with two permeant species were expanded in full, there would be a sum of 16 terms each made of the product of six rate constants. Heckmann et al. (1969) discuss a partial solution for the same barrier model but operating in single-file mode with one permeant species as represented by the diagram of Fig. 2 C. Each R now has several hundred products of seven rate constants. If that single-file pore is restricted either to never being empty (no state OOO) or instead to never being full (no state AAA), each R is reduced to the sum of 96 products of six rate constants. Despite the complexity of these equations, it is still practical to calculate current-voltage relations with a digital computer. However, to discuss ionic selectivity or even tracer flux ratios with such single-file models requires including a second permeant species and adding thousands of terms to the R expressions. Such systems might be more readily solved by Monte Carlo methods or by direct computer simulation (Baker, 1971).

METHODS

The object of the experiments was to record the peak current-voltage (I-E) relations for current in Na channels when the nerve membrane was bathed in different external solutions. The ratio of peak currents measured at each membrane potential but in two different external solutions was compared with the ratio of currents predicted by the one-ion pore model. The implicit assumption is made that changes in the current are due to differences in the rates and probabilities of transit of different ions through open channels rather than to any "opening" or "closing" actions of bathing ions on gating mechanisms. In several cases this simplification is manifestly incorrect.

Many of the experiments reported here were done in the period 1970–1972 in conjunction with measurements of the ionic selectivity of the Na channel of frog myelinated nerve (Hille, 1971, 1972). The methods are described in those papers. Briefly ionic currents of single myelinated fibers were measured with the voltage clamp method of Dodge and Frankenhaeuser (1958). The membrane was ordinarily held

at − 80 mV and depolarized in brief steps. Test pulses were preceded by 40–60-ms prepulses to −125 mV to eliminate short-term sodium inactivation. Currents in K channels were blocked by the inclusion of a tetraethylammonium salt in the external solution, and the peak current in Na channels was determined after subtracting leak and capacity currents. The tested salts used are listed in earlier papers (Hille, 1971, 1972). Isotonic external solutions contained 2 mM $CaCl_2$, 1–4 mM trishydroxymethylaminomethane-HCl buffer at pH 7.4, 6 mM tetraethylammonium Br or NO_3, and 110–116 mM monovalent test salts. Hypertonic solutions were made by including a higher concentration of test salts in the solution. The ends of the fibers were cut in 120 mM KCl or 120 mM CsF. Sodium ion activities were measured with a Corning No. 476210 Na-sensitive glass electrode (Eisenman et al., 1957) Corning no. 476210 (Corning Glass Works, Corning, N. Y.) against a Beckman No. 39402 ceramic junction, saturated-KCl reference electrode (Beckman Instruments, Fullerton, Calif.). Experiments were done at a fixed temperature of 5°C.

RESULTS

Properties of the One-Ion pore Model

Before examining experimental results, it is helpful to describe how the parameters of the model affect predicted fluxes. The one-ion pore model with four barriers actually has far more free parameters than can be determined in the experiments to be discussed. Therefore all but two parameters have been fixed at tentative values giving reasonable results as listed in Table I and then experimentally observed ionic selectivities and deviations from independence are fitted by adjusting the two remaining parameters. These two parameters are the depth of well 2 and the height of barrier 23, features of the energy profile that are henceforth often referred to as the "external binding site" and the "selectivity filter." The values chosen for $G2$ and $G23$ are summarized in Table II.

The two free parameters $G2$ and $G23$ may be chosen independently without difficulty. As was already discussed, only energy peaks and not energy valleys determine ionic fluxes and zero-current potentials for pores satisfying independence (see Eq. 3). It can also be shown that zero-current potentials (but not fluxes) in one-ion pores have exactly the same values as for the cor-

TABLE I

STANDARD PARAMETERS FOR MODEL WITH Na^+ ION

Valley energies	Barrier energies	Electrical distances
$G2 = -1$	$G12 = 6$	$2 \cdot D1 = 0.27$
$G3 = 0.5$	$G23 = 9$	$2 \cdot D2 = 0.23$
$G4 = 0.5$	$G34 = 7$	$2 \cdot D3 = 0.25$
	$G45 = 7$	$2 \cdot D4 = 0.25$

Energies given in units of RT.

TABLE II

PROPERTIES OF THE BINDING SITE AND SELECTIVITY FILTER

Ion	*G23*	*G2*	K_{diss}*
	RT	*RT*	*mM*
Na^+	9.0	−1.0	368
Li^+	9.1	−1.8	165
Tl^+	10.4	−3.0	50
K^+	11.7	−1.5	220
Rb^+	>13.7	−1.5	220
Cs^+	>13.7	−1.5	220
NH_4^+	11.1	−1.0	368
Formamidinium	11.2	−2.3	100
Guanidinium	11.3	−2.1	122
OH-guanidinium	11.4	−2.6	74
H^+	?	−12.6	0.003

* K_{diss} is the apparent dissociation constant of state 2 at 0-mV potential.

responding pore with independence (Läuger, 1973; Hille, 1975 *b*). Therefore, the depth of energy valleys has no influence on reversal potentials even in the one-ion pore. Since *G*23 is the only energy peak height free to be varied, its value for each ion may be chosen at once from selectivity ratio measurements using zero-current potential (Hille, 1971, 1972). Then the value of *G*2 can be chosen to fit any measured deviation from independence as explained in the next paragraph.

In the model, deviations from independence arise from saturation of pores by ion binding. The binding process is complicated, because for each ion species there are three possible bound states of the pore (Fig. 2 B). Equilibrium binding will be strongest to the site with the deepest energy well, site 2. Thus state 2 is the most probable of the bound states. From conventional thermodynamics, the equilibrium dissociation constant K_{diss} of state 2 with zero applied field is simply exp(*G*2). Values of K_{diss} calculated this way are listed in Table II. For Na^+ ions the value of *G*2 best describing experimental results (see later) is $-1.0\ RT$ (Table II). Thus with an internal and external sodium concentration of exp(−1.0) or 0.368 M and with 0 mV potential, the number of pores in occupied state 2 equals the number in free state 1. The complete distribution among states 1 through 4 with 368 mM Na^+ is actually 0.41, 0.41, 0.09, and 0.09. Moreover, even when the internal Na^+ is removed, the fraction of channels in state 2 remains almost equal to that in state 1 for 0.368 M external sodium, because barrier 23 is so high relative to barrier 12 that equilibrium from the external compartment is dominant.

The partial saturation of pores reduces the possible fluxes in the pore because of the one-ion restriction. The probability that an ion will cross the

membrane decreases when other ions are added exactly in proportion to the decrease in the probability of finding an unoccupied channel. Therefore once $G23$ has been chosen to fit reversal potential measurements, $G2$ may be chosen to fit the amplitude of observed currents. In the model, the external binding site for permeant ions is assumed to be the same as the binding site for H^+ described by Hille (1968) and Woodhull (1973). The "electrical distance" $2 \cdot D1$ from the outside to site 2 has been set at 0.27 to match the observed voltage dependence of block by H^+ ions (Woodhull, 1973).

As was already stated, the four-barrier model is more complex than is needed to discuss competition of externally applied ions. Indeed current ratios in the experiments to be described can be fitted by a two-barrier model. A more complicated model was chosen for several reasons. First, two-barrier models fitted to the experiments give hyperlinear current-voltage relations curving up at positive internal potentials where the current-voltage relation of open Na channels is usually convex. Second, there already is evidence from experiments with internal perfusion (e.g., Chandler and Meves, 1965) that internal ions can block Na channels. Such phenomena could be described by adding a binding site closer to the axoplasm than the selectivity filter. Since internal block will probably be investigated soon, the appropriate terms were included in the model. Until then the values chosen for the parameters $G3$, $G34$, $G4$, $G45$, $D3$, and $D4$ have to be regarded as somewhat arbitrary. The following paragraphs explain the preliminary choice of values for these parameters as well as for the absolute value of $G23$Na.

The few properties of Na channels that help to give limits to the remaining parameters are the temperature coefficient of the maximum conductance, the conductance of a single open channel, and the shape of the "instantaneous" I-E relations of an open channel. These properties are considered one at a time. The Gibbs free energy change ΔG for any process at constant temperature is composed of enthalpic and entropic terms: ΔH-$T\Delta S$. By inserting these terms into Eq. 1 it can be seen that only the enthalpic part enters into the temperature coefficient. If the barrier heights given in Tables I and II are assumed to be entirely enthalpies, then the temperature coefficient (Q_{10}) of net Na^+ flux at 0 mV is 1.34 between 0 and 10°C and 1.33 between 10 and 20°C. These values are within the 1.3–1.5 range of experimental observations on axons (Hodgkin et al., 1952; Frankenhaeuser and Moore, 1963; Schauf, 1973). The single-channel chord conductance of the model pore with 120 mM external Na^+ and 12.5 mM internal Na^+ is 128 pmho at 0 mV. This value is in line with early estimates of Na channel conductance based on indirect conclusions from nerve bundles (Hille, 1970) but not with more recent lower estimates based on somewhat more direct measurements with squid giant axons and frog muscle fibers (Armstrong and Bezanilla, 1973; Keynes and Rojas, 1974; Almers and Levinson, 1975; Keynes et al., 1975;

Levinson and Meves, 1975). The newer estimates would be better fitted by adding an entropic contribution equivalent to 4 RT to each barrier peak, thus for example bringing G23Na from 9 to 13 RT. The single channel conductance then falls to 2.3 pmho. The Q_{10}, binding, and selectivity properties would not be affected by this change. In conventional thermodynamic terms the added entropy change is -8 entropy units (calorie degree^{-1} mole^{-1}). However even if a perfect fit could be made to all known properties of Na channels, the model must be regarded as an empirical description hopefully giving helpful insight into underlying factors, but not providing exact values of physical variables.

Under normal ionic conditions the I-E relation of open Na channels fits Ohm's law in squid giant axons (Hodgkin and Huxley, 1952 *b*) and the constant field flux equation in frog and toad myelinated nerve (Dodge and Frankenhaeuser, 1958, 1959). The I-E relation of the standard one-ion pore, shown as open circles in Fig. 4, is intermediate between the lines for Ohm's law and the Goldman-Hodgkin-Katz equation. The circles actually represent the indistinguishable results of two separate calculations, one with 12.5 mM Na^+ as the only internal permeant ion and one with 120 mM K^+ as the only internal permeant ion. The calculated I-E relation can be made linear or more curved by several different modifications of the standard parameters. Frankenhaeuser (1960) has shown how to do this with internal or external surface potentials, and Woodbury (1971), with gradations of barrier height. Two other simple changes are equally effective in increasing the curvature. The solid triangles in Fig. 4 give the I-E relation with 120 mM K^+ inside and

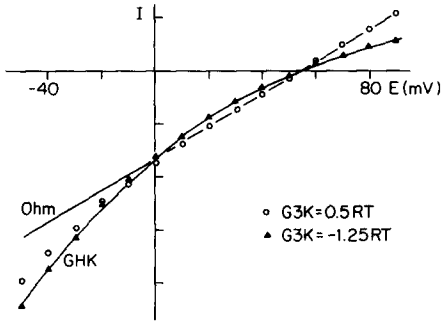

FIGURE 4. Current-voltage relations of the one-ion pore model compared with Ohm's law (Ohm) and the Goldman-Hodgkin-Katz flux equation (GHK). For open circles, the standard parameters (Table I) were used with only one permeant species: C1Na = 120 mM, C5Na = 12.5 mM. Same results were obtained with two permeant species: C1Na = 120 mM, C5K = 120 mM. For solid triangles: $G3 = -1.25\ RT$, C1Na = 120 mM, C5K = 120 mM. Same results were obtained with: $2 \cdot D3 = 0.50$, $2 \cdot D4 = 0$, C1Na = 120 mM, C5Na = 12.5 mM. I-E relations in each case were scaled by factors from 1 to 1.25 to make them match. The current scale marks correspond to 4–5 pA per channel.

with $G3K$ set equal to $-1.25\ RT$. The change makes valley 3 into an "internal binding site" with a dissociation constant of 287 mM and gives *I-E* relations indistinguishable from the Goldman-Hodgkin-Katz theory. A second way to get the same curvature with 12.5 mM Na^+ inside is to set $2 \cdot D4$ equal to zero, $2 \cdot D3$ equal to 0.50, and $G45Na$ equal to $8\ RT$. This removes the electric field as a driving force over the innermost barrier, so at high positive potentials diffusion of ions from axoplasm to valley 4 becomes rate limiting. There seems to be no point in refining the predicted *I-E* relations further until experimental evidence gives some clue to which of many possible changes of parameters is appropriate.

As was already discussed, the barrier heights for different permeant species have to obey the constant offset energy condition (Eq. 4) if the model is to satisfy the Goldman-Hodgkin-Katz voltage equation exactly. Since the one-ion pore described here is assumed to have only one selectivity filter and the other barriers stay constant, Eq. 4 is not obeyed and the familiar voltage equation does not hold strictly. Put another way, applying the Goldman-Hodgkin-Katz voltage equation to reversal potentials calculated with the model will give permeability ratios that themselves depend on the conditions of the calculation. An example is given in Table III. Here the reversal potential has been calculated in the model for four sets of ionic conditions involving Na^+ and K^+ ions. The last two columns give selectivity ratios P_K/P_{Na} calculated from the reversal potentials of the model using the Goldman-Hodgkin-Katz equation. The column labeled "from E_{rev}" is calculated from absolute reversal potentials as in the experiments of Chandler and Meves (1965), while the column labeled "from ΔE_{rev}" is calculated from changes in reversal potentials on changing external solutions as in the experiments of Hille (1971, 1972). Both methods of calculation give results depending on the "experimental" conditions.

With this preliminary description of the properties of the model, we turn

TABLE III

REVERSAL POTENTIALS AND VARIABLE SELECTIVITY RATIOS IN THE ONE-ION PORE

	Assumed ionic concentrations					P_K/P_{Na}	
Case	$[Na]_o$	$[Na]_i$	$[K]_o$	$[K]_i$	E_{rev}	From E_{rev}	From ΔE_{rev}
	mM	*mM*	*mM*	*mM*	*mV*		
1	120	12.5	0	0	54.11	—	—
2	120	0	0	120	54.29	0.104	—
3	0	12.5	120	0	−4.59	0.086	0.087*
4	0	0	120	120	0.00	—	0.104‡

* Case 3 minus case 1.

‡ Case 4 minus case 2.

to showing that many experimental observations on nodes of Ranvier can be understood better by flux equations of the saturating one-ion pore than by flux equations derived from free diffusion.

Na^+ Currents in Nerve Do Not Fit Independence

Fig. 5 shows peak *I-E* relations (symbols) measured on a node of Ranvier bathed with external isotonic solutions containing ⅛, ¼, ½, and 1 times the

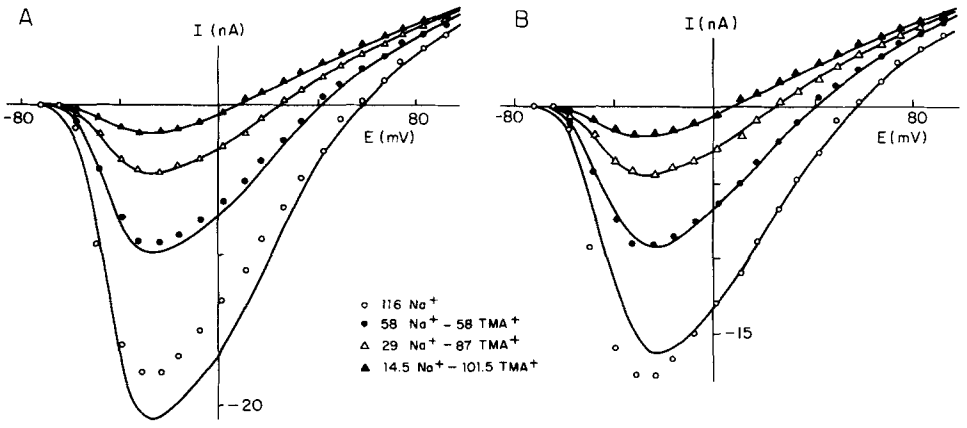

FIGURE 5. Peak *I-E* relations of a node bathed in various isotonic mixtures of NaBr and tetramethylammonium Br compared with smooth curves derived from the independence relation (A) and from the one-ion pore model (B). Concentrations of major ions are given in millimolar units. Ends of fiber cut in KCl. Assumed value of $C5Na$ = 11.2 mM. (Data from Fig. 10 of Hille, 1975 *b*.)

normal Na^+ concentration. Impermeant tetramethylammonium (TMA) ion is used to keep the ionic strength constant. As the Na^+ concentration is increased, inward currents and the zero-current potential both increase, as they should if Na^+ is the charge carrier. Similar changes are seen in the experiment of Fig. 6 with solutions of double the normal tonicity containing ½, 1, and 2 times the normal Na^+ concentration. The smooth curves in Figs. 5 A and 6 A are calculated from the familiar independence relation (Hodgkin and Huxley, 1952 *a*), which is in the present notation

$$\frac{M\mathrm{Na}'}{M\mathrm{Na}''} = \frac{C1\mathrm{Na}' - C5\mathrm{Na}' \cdot \exp(\mathrm{V})}{C1\mathrm{Na}'' - C5\mathrm{Na}'' \cdot \exp(\mathrm{V})}, \tag{5}$$

where primes and double primes represent the two conditions compared. In calculating the curves it is assumed that the inside concentration $C5Na$ does not change as $C1Na$ is changed. The measurements with 14.5 or 29 mM Na^+ are used as reference curves and the other curves are calculated. The curves

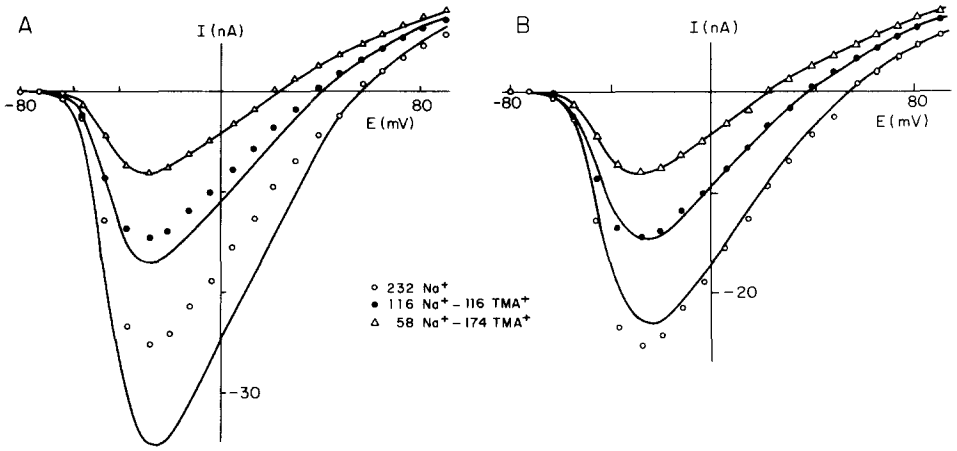

FIGURE 6. Peak *I-E* relations of a node bathed in twice hypertonic mixtures of NaCl and TMA Cl compared with smooth curves derived from the independence relation (A) and from the one-ion pore model (B). Ends of fiber cut in KCl. Assumed value of $C5Na$ = 24 mM. (Data from Fig. 11 of Hille, 1975 *b*.)

and experiments do not agree. As Na^+ concentration is increased, measured inward currents grow less than the independence relation predicts. Evidently the probability that a Na^+ ion crosses the channel decreases as other Na^+ ions are added to the external solution. Essentially the same result was obtained in over 20 repeats of the same experiment. The result did not depend on whether the Na^+ and TMA salts were chlorides, bromides, or nitrates. Parenthetically, varying the anion did produce a clear shift of the voltage dependence of opening of Na channels. Relative to Cl^-, the shift in Br^- was -4 to -7 mV and in NO_3^-, -11 to -15 mV, both in the direction equivalent to reducing the calcium concentration.

Before discussing the observations in terms of saturation, the possibility needs to be considered that the TMA ion might raise the activity coefficient of Na^+ ions or somehow enhance the permeability of Na channels to Na^+ ions. Both explanations can be ruled out by measurements of Na^+ currents with other mixtures of Na^+ and TMA ions. In one test, peak inward Na^+ currents with an external solution containing 58 mM Na^+ and 58 mM TMA were not significantly (5%) larger than with a solution containing 58 mM Na^+ and 116 mM sucrose. In several tests, the recorded maximum peak Na^+ current increased only 10% as an isotonic solution with 116 mM Na^+ was replaced by a twice hypertonic solution containing 116 mM Na^+ and 116 mM TMA. The small apparent increase may be an artifact of fiber shrinkage increasing the resistance of the current recording path in the fiber, and, in any case, is nowhere near the magnitude needed to explain the observations of Figs. 5 and 6 by mechanisms involving effects of TMA ions. Relative activities of Na^+ were also measured with a Na-selective glass electrode. Activity

changes upon adding TMA ions were simply those expected from the calculated increases of ionic strength.

The barrier model of a one-ion pore can explain the observed deviations from independence. A value for the binding energy $G2Na$ must first be selected by trial and error to give the appropriate saturation of pores as the external Na^+ concentration is increased. The smooth curves in Figs. 5 B and 6 B are calculated using the model and parameters in Table I to find current ratios in the same way as with the independence relation. As before, measurements in 14.5 or 29 mM Na^+ are used for the reference curve, and the effective internal ion concentrations are assumed not to change. The saturating model gives an improved fit relative to the independence relation. Some residual deviations at internal potentials more negative than −20 mV might be partly attributable to changes in the number of open Na channels due to changes in the series resistance artifact and to direct effects of ionic concentrations on gating. In the calculations given here and in Figs. 6–8 the internal permeant ions are always represented by an equivalent quantity of Na^+ picked to match the observed reversal potential. The assumed concentration $C5Na$ is given in the figure legends. Other ions like K^+ may actually be more important than Na^+ in carrying current in several experiments, but internal concentrations are not known. Repeating the calculations assuming that K^+ is the permeant ion does not change the conclusions of this paper significantly. In the calculation of Fig. 5 B, the proportion of free channels (state 1) at 0 mV is 0.95, 0.91, 0.85, and 0.74 in the successively higher external Na^+ concentrations. With 120 mM Na^+ the complete distribution of channels among states 1 through 4 at 0 mV is 0.74, 0.23, 0.015, and 0.010.

Permeant and Impermeant Ions Block Na Channels

Most of the ions tested previously as sodium substitutes reduced currents in Na channels more than theories like the Goldman-Hodgkin-Katz formalism predict (Hille, 1971, 1972). If PA and PB are the permeabilities to monovalent ions A and B, then the current ratio on changing from a solution of pure A outside to a mixture is in such theories

$$\frac{I'}{I''} = \frac{P\mathrm{A}\cdot[C1\mathrm{A}' - C5\mathrm{A}\cdot\exp(V)]}{P\mathrm{B}\cdot C1\mathrm{B}'' + P\mathrm{A}\cdot[C1\mathrm{A}'' - C5\mathrm{A}\cdot\exp(V)]} = \frac{C1\mathrm{A}' - C5\mathrm{A}\cdot\exp(V)}{(C1\mathrm{A}'' + C1\mathrm{B}''\cdot P\mathrm{B}/P\mathrm{A}) - C5\mathrm{A}\cdot\exp(V)}. \quad (6)$$

The ratio is like the independence relation (Eq. 5) and may be called the extended independence relation. If it is obeyed, adding a concentration $C1$B of ion B should be indistinguishable from adding a concentration $C1\mathrm{B}\cdot P\mathrm{B}/P\mathrm{A}$ of ion A. Although the ions are changed, the entire current-voltage curve would stay the same. In the first experiments with Na^+ substitutes, the fre-

quent depression of currents relative to the predictions of Eq. 6 was regarded as a simple "anesthetic" action of the ions on the membrane. However with guanidinium compounds, and even more so with thallous ions, the depression had the obvious interesting property of being less evident with stronger depolarization, i.e., the curvature of the current-voltage relation changed. This led to the impression that the binding site involved might be within the channel and part way across the potential drop in the membrane. Then the probability that an ion pauses at that site would depend on the membrane potential as well as on the concentration of the ion. These ideas were first put in quantitative form in Woodhull's (1973) rate theory model for voltage-dependent block of Na channels by H^+ ions. The success of that work inspired this attempt to explain voltage-dependent block and permeation of ions all in one self-consistent theory.

Fig. 7 A and B give examples of deviations from Eq. 6 with guanidinium compounds. In each case ionic substitutions are made that, according to Eq. 6, should not have a detectable effect on the peak *I-E* relation. As expected, the substitutions change the reversal potentials (zero-current potentials) only slightly. However, both in Fig. 7 A where pure hydroxyguanidinium replaces Na^+ and in Fig. 7 B where a mixture of guanidinium and Na^+ replaces Na^+, the guanidinium ions depress the net current flowing in either direction. Unlike the effect of tetrodotoxin, for example, the depression is voltage dependent, being much less for the largest depolarizations than for depolarization to 0 mV. The fair fit of the smooth curves in the figure shows that partial saturation of site 2 in the one-ion pore gives a reasonable explanation for simultaneous blocking and current-carrying properties of guanidinium compounds. As can be seen from the dissociation constants in Table II, the binding of guanidinium compounds is much stronger than the binding

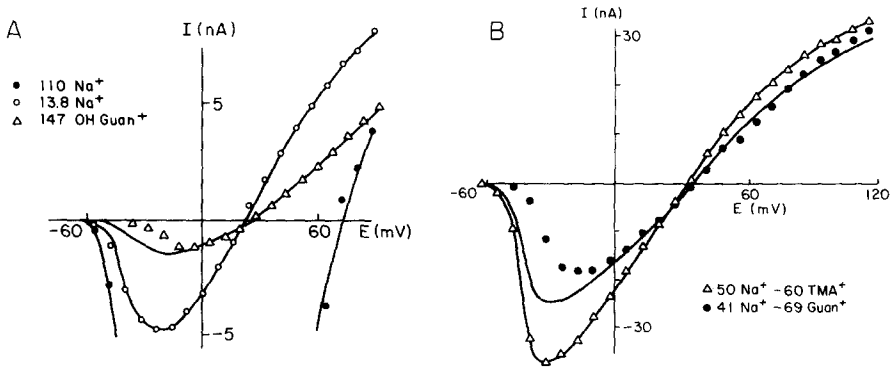

FIGURE 7. Peak *I-E* relations in hydroxyguanidinium sulfate Ringers' and in mixed NaCl-guanidinium *Cl* Ringers' compared with smooth curves derived from the one-ion pore model. (A) Ends of fiber cut in CsF. Assumed value of *C*5Na = 5.7 mM. (Data from Fig. 6 of Hille, 1971.) (B) Assumed value of *C*5Na = 13 mM.

of Na^+ ions. Some deviation of the fitted curves from the observations with very small depolarizations suggests that guanidinium compounds may also have a calcium-like action on the voltage-dependent opening of Na channels.

Similar experiments in Fig. 8 show that thallous ions combine blocking and current-carrying properties. In Fig. 8 A, external 110 mM Tl^+ gives about the same reversal potential as 40 mM Na^+ but smaller inward currents than 13.8 mM Na^+. In Fig. 8 B, adding 58 mM Tl^+ to 58 mM Na^+ increases the reversal potential but decreases the net inward current relative to a mix-

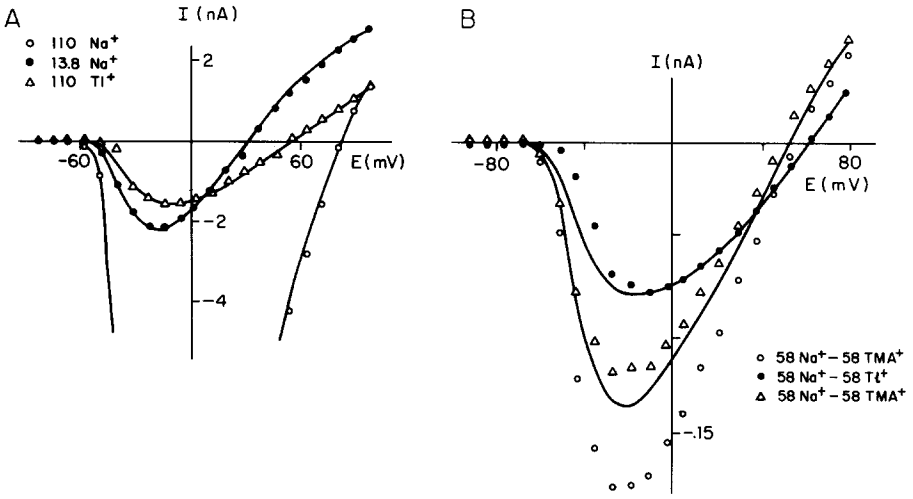

FIGURE 8. Peak *I-E* relations with mixtures of $TlNO_3$, $NaNO_3$, and TMA NO_3. Ends of fiber cut in CsF. (A) Small Tl^+ currents in 110 mM Tl^+. Assumed value of $C5Na$ = 4.0 mM. (Data from Fig. 5 of Hille, 1972.) (B) Block of Na^+ + Tl^+ currents by Tl^+. Open circles before and triangles after exposure to Na^+ + Tl^+ solution. Assumed value of $C5Na$ = 6.6 mM. (Data from Fig. 12 of Hille, 1975 *b*.)

ture of 58 mM tetramethylammonium ion with 58 mM Na^+. Again the changes are reasonably fitted by smooth curves calculated from the one-ion pore model assuming a dissociation constant at 0 mV of 50 mM for Tl^+ ions from site 2. Even the evident voltage dependence of the block is well described, except once more for the smallest depolarizations where Tl^+ ions, like guanidinium ions may have a small calcium-like effect on opening of channels. The poor reversal of the experiment in Fig. 8 B is typical of the quickly developing toxic effects of Tl^+ and makes an unambiguous comparison of theory with experiment impossible. Complete recovery was never obtained, and, as in this case, the leaky node often gained Na^+ rapidly during the wash period.

While thallous and guanidinium ions are the two permeant ions with the most obvious channel-blocking effects, many other small ions also blocked to some degree. For example in Li^+ Ringer's the reversal potential is nearly the

same as in Na^+ Ringer's but the inward currents at −20 mV are 28% smaller (Hille, 1972). The effect is well fitted by assuming an apparent dissociation constant of 165 mM for the complex of site 2 with Li^+ ions at 0 mV. With ions of low permeability, two kinds of experiments were done to measure block. The sizes of inward currents were compared in 1:1 mixtures of Na^+ Ringer's with Na^+-free Ringer's made with TMA, sucrose, choline, K^+, Rb^+, and Cs^+, and the sizes of outward currents in pure TMA Ringer's were compared with outward currents in Ringer's made entirely with other nearly impermeant ions. Some derived parameters are given in Table II and others are simply listed here. Replacing TMA with impermeant sucrose, choline, and methylammonium did not change inward or outward currents. Presumably none of these substances binds appreciably to the Na channel. Replacing 55 TMA with K^+, Rb^+, or Cs^+ depresses inward Na^+ currents at 0 mV by 15–20% as if these ions bind to the channel slightly more strongly than Na^+ ions with a K_{diss} of 140–250 mM. The same values of K_{diss} were obtained replacing 110 mM TMA by these ions and measuring outward currents. Replacing 110 mM TMA with formamidinium or acetamidinium depressed outward currents at +75 mV by 25% as if these ions bind with a K_{diss} of 80 mM. Finally replacing 110 mM TMA with methylguanidinium (see Fig. 6, Hille, 1971), triaminoguanidinium, Tris, or imidazole depressed outward currents at +75 mV by 38–47%, as if these ions bind with a K_{diss} of 27–40 mM. All the organic ions that depressed ioic currents showed clear voltage dependence of the bock of the same type as the model predicts for ions binding to site 2 in the energy profile (Fig. 1). With K^+, Rb^+, and Cs^+ there seemed to be a calcium-like shift of the activation of channels, but the depression of currents was too small to allow voltage dependence of block to be studied.

DISCUSSION

Permeability and the Usefulness of the One-Ion Model

Flux equations based on continuum electrodiffusion theory have played an essential role in developing the ionic hypothesis. However they fail when ionic concentrations are made high enough to saturate sites within ionic channels. The electrodiffusion theory has only one free parameter per ion, the permeability. By introducing saturation and a second free parameter, a binding constant, the one-ion pore model can deal with saturation from externally applied ions. A third free parameter, again a binding constant, would be needed to deal with saturation at internal binding sites. The two-parameter theory was adequate to fit the major deviations from independence in the experiments described here. The residual deviations in the experiments of Figs. 5–8 may tentatively be ascribed to changes in the voltage dependence of gating with different ions rather than to the properties of open channels.

In the modern literature the ionic permeability of a membrane is measured

in three distinct ways: tracer flux measurements, conductance or current amplitude measurements, and zero-current potentials. It is well known that permeabilities derived from tracer flux and conductance do not agree when there is flux coupling, as in a single-file mechanism or in exchange diffusion (see, e.g., Hodgkin and Keynes, 1955). My experiments on Na channels (Hille, 1971, 1972) show that permeabilities derived from conductance and zero-current potentials also need not agree and that the two methods may even give selectivity sequences in the opposite order. This problem arises when ions do not move independently and is discussed in more detail elsewhere (Hille, 1975 *b*). Since we will undoubtedly continue to use the word "permeability" to describe several different operationally defined membrane properties, there is certain to be confusion unless the imprecision of the word is widely recognized. Whenever biophysical arguments are made using permeability properties, the method of measurement will need to be taken into account. Models of the kind described in this paper can be used in discussing all three types of permeability data.

Similar but less completely developed saturating models have already been described in the literature (Heckmann et al., 1972; Läuger, 1973; Woodhull, 1973; Chizmadjev et al., 1974; Markin and Chizmadjev, 1974). Like the present model (Fig. 3), each of these leads to flux equations that are too complex to be preferred over the Goldman-Hodgkin-Katz flux equations except when deviations from independence are obvious. The fair fit of the one-ion model to experiments must mean that saturation of sites can play a significant role in Na channels but is not proof that only one ion is allowed at a time. Multiion models can be constructed that have many of the properties of one-ion models, plus some additional ones. Indeed in several unpublished experiments on fibers with ends cut in NaCl and bathed in guanidinium and Na^+ ion mixtures, results were obtained that were easiest to explain by multi-ion models. In these experiments outward Na^+ currents actually decreased with increasing depolarization at high positive voltages when the node was bathed in high external Na^+. Replacing some of the external Na^+ by guanidinium removed this negative slope resistance, so that outward Na^+ currents became larger than in the pure Na^+ medium. The present model gives isotopic (unidirectional) flux ratios satisfying the Ussing (1949) flux ratio criterion exactly, while multiion models often would not. Hopefully further attempts to measure isotopic flux ratios in Na channels will be made to clarify what degree of flux coupling exists in Na channels.

Deviations from Independence with Na^+ Ions

There are not many previous tests of the independence relation for comparison with the studies reported here. In the squid giant axon Hodgkin and Huxley (1952 *a*) concluded that Na currents change as predicted when external Na^+ concentration was lowered. However, the measured currents with progressively

lowered Na^+ were actually 20, 33, and 60% larger than expected, an effect attributed to changes in the degree of inactivation of Na channels at rest. While the Na channel of the squid giant axon certainly is not half-saturated at 368 mM Na^+ (the value for the node), a K_{diss} of 1 M could easily be accommodated within the uncertainty of the corrections applied in the experiment of Hodgkin and Huxley. The experiment could be repeated using prepulses to eliminate sodium inactivation as an adjustable parameter. Chandler and Meves (1965) reversed the experiment by placing Na^+ inside squid giant axons. Currents obtained on replacing internal 300 mM KCl by 150 mM KCl + 150 mM NaCl were significantly smaller than predicted by the independence principle. The deviations were voltage dependent. Their results could be reasonably fitted by postulating an internal binding site at an "electrical distance" of 0.3 from the inside of the axon and with a K_{diss} of 750 mM for Na^+ ions.

In the node of Ranvier of the frog, Dodge and Frankenhaeuser (1959) show one experiment agreeing perfectly with the independence relation as external Na^+ is lowered to 37% of normal. Again prepulses were not used, but it would be difficult to prove that there was some error that exactly cancelled deviations from independence in their experiment. In the Goldman-Hodgkin-Katz theory the slope conductance of a Na channel is predicted to increase linearly with external Na^+ concentration if the measurements are made at a fixed voltage, but the conductance with no external Na^+ is not zero since internal Na^+ ions contribute to slope conductance. Two groups have reported experimental measurements of peak sodium conductance with changes of Na^+ concentration, but overlooked the necessity of residual conductance with no external Na^+ in the analysis. Dubois and Bergman (1971 *a,b*) fitted conductance observations in iso- and hypertonic solutions to a Michaelis-Menten relationship, finding a voltage-dependent K_{diss} near 150 mM at 0 mV. The phenomena they report seem to be closely related to those described here. Drouin and Neumke (1974) measure the maximum chord conductance without regard to voltage and report no evidence of saturation with isotonic solutions.

Molecular Interpretation of the Model

In earlier papers from this laboratory, a negative carboxylic acid group lying in an oxygen-lined slit was proposed for the structure of the selectivity filter (Hille, 1971, 1972). This paper shows that the filter can be treated as an energy barrier immediately preceded by a binding site. The diagram of Fig. 9 shows how a carboxylic acid might have this property. The arriving cation is fully hydrated in the external solution, position 1. As it approaches the carboxylic acid oxygen O1 of the selectivity filter, the ion loses a small number of water molecules but is stabilized energetically by its attraction to the negative charge of O1. This is the bound state, state 2. Then as the ion,

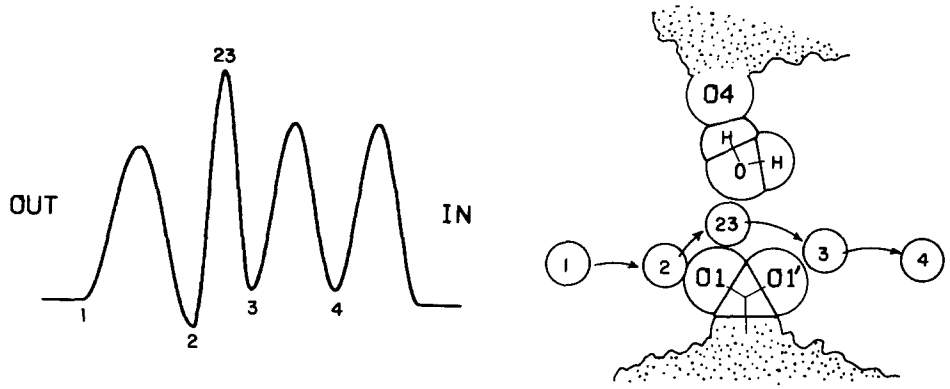

FIGURE 9. Molecular interpretation of the binding site and selectivity filter in the one-ion pore model. The ion is shown as a circle with the crystal size of Na^+ advancing from position 1 to position 4. The fixed part of the selectivity filter includes the oxygens O1 and O1′ of the carboxylic acid group and oxygen O4 drawn to scale. A mobile water molecule HOH is shown temporarily hydrogen bonded to O4. The ion in position 23 is in the highest energy state where it can be in contact with the smallest number of water molecules. (After Hille, 1972, 1975 *c*.)

still in contact with O1, enters the narrow 3 × 5-Å selectivity filter, many more water molecules must be shed and a high energy "transition complex" labeled 23 is formed. The selectivity measurements based on reversal potentials and the speculations on the electrostatic origin of the underlying forces in previous papers (Hille, 1971, 1972) all pertain to the nature of this high energy complex. The energy of the complex differs from ion to ion and hence the channel is selective. The ion then moves on through the narow region, regaining some water molecules to form state 3. Finally state 4 and the axoplasmic state are reached by further jumps over energy barriers no higher than those for aqueous diffusion.

As drawn, the physical distance of travel needed to pass through the high energy state is much more than is normally associated with a single activated complex. Therefore, the barrier forming the selectivity filter might better be drawn as a broader high energy plateau with several small valleys in it. However, these kinds of refinements are quite unnecessary for successful modeling and would have little effect on the results. The drawing also suggests that state 3 might be a bound state chemically quite similar to state 2. In that case the energies $G3$ should be made lower than in the parameter set used here. Experiments with internally perfused giant axons would help determine the appropriate values.

Specialization of Na Channels

The open Na channel may be regarded as a catalyst designed to promote the flux of Na^+ ions across the nerve membrane with high ionic specificity and without interference from other naturally occurring ions. These goals seem

well fulfilled. Table II shows that, of all tested ions, Na^+ ions bind the least and pass the best through the channel. The external binding site has an apparent K_{diss} of 20 mM for Ca^{++} ions (Woodhull, 1973), 150 mM for K^+ ions, and 3 μM for H^+ ions. Each value of K_{diss} is well above the normal external concentration of the ion, so external competition from these ions will not be important. In addition, the 12:1 selectivity against K^+ ions is probably as high as is useful to make a positive reversal potential, since the sodium pump is limited in how large an Na gradient it can maintain. Finally, as Fig. 9 is meant to imply, it is possible that through an hour glass-shaped structure all the transmembrane potential drop and the barriers to ion flow are concentrated in a stretch of 5 Å in the channel so the flux rates are much greater than could be achieved by a long narrow pore.

I thank Drs. W. Almers, D. T. Campbell, and T. Begenisich for commenting on a draft of the manuscript and Susan A. Morton for valuable secretarial help.
This work was supported by grants NS08174 and RR0374 from the National Institutes of Health.

Received for publication 19 March 1975.

REFERENCES

ALMERS, W., and S. R. LEVINSON. 1975. Tetrodotoxin binding to normal and depolarized frog muscle and the conductance of a single sodium channel. *J. Physiol.* (*Lond.*). In press.

ARMSTRONG, C. M. 1971. Interaction of tetraethylammonium ion derivatives with the potassium channels of giant axons. *J. Gen. Physiol.* **58**:413–437.

ARMSTRONG, C. M., and F. BEZANILLA. 1973. Currents related to movement of the gating particles of the sodium channels. *Nature* (*Lond.*). **242**:459–461.

BAKER, M. 1971. Ion transport through nerve membranes. Ph. D. Thesis. University of Washington, Seattle. University Microfilms, Ann Arbor, Michigan.

BEZANILLA, F., and C. M. ARMSTRONG. 1972. Negative conductance caused by entry of sodium and cesium ions into the potassium channels of squid axons. *J. Gen. Physiol.* **60**:588–608.

CHANDLER, W. K., and H. MEVES. 1965. Voltage clamp experiments on internally perfused giant axons. *J. Physiol.* (*Lond.*). **180**:788–820.

CHIZMADJEV, Y. A., B. I. KHODOROV, and S. K. AITYAN. 1974. Analysis of the independence principle for the sodium channels of biological membranes. *Bioelectrochem. Bioenergetics.* **1**:301–312.

DODGE, F. A., and B. FRANKENHAEUSER. 1958. Membrane currents in isolated frog nerve fibre under voltage clamp conditions. *J. Physiol.* (*Lond.*). **143**:76–90.

DODGE, F. A., and B. FRANKENHAEUSER. 1959. Sodium currents in isolated frog nerve fibre of *Xenopus laevis* investigated by the voltage clamp technique. *J. Physiol.* (*Lond.*). **148**:188–200.

DROUIN, H., and B. NEUMCKE. 1974. Specific and unspecific charges at the sodium channels of the nerve membrane. *Pfluegers Arch. Eur. J. Physiol.* **351**:207–229.

DUBOIS, J-M., and C. BERGMAN. 1971 *a*. Variation de la conductance sodium de la membrane nodale en fonction de la concentration en ions Na^+. *C. R. H. Acad. Sci.* **272**:2796–2799.

DUBOIS, J-M., and C. BERGMAN. 1971 *b*. Conductance sodium de la membrane nodale: inhibition compétitive calcium-sodium. *C. R. H. Acad. Sci.* **272**:2924–2927.

EISENMAN, G., D. O. RUDIN, and J. U. CASBY. 1957. Glass electrode for measuring sodium. *Science* (*Wash. D.C.*). **126**:831–34.

EYRING, H., R. LUMRY, and J. W. WOODBURY. 1949. Some applications of modern rate theory to physiological systems. *Rec. Chem. Prog.* **10**:100–114.

FRANKENHAEUSER, B. 1960. Sodium permeability in toad nerve and in squid nerve. *J. Physiol.* (*Lond.*). **152**:159–166.

FRANKENHAEUSER, B., and L. E. MOORE. 1963. The specificity of the initial current in myelinated nerve fibres of *Xenopus laevis*. *J. Physiol.* (*Lond.*). **169**:438–444.

FROST, A. A., and R. G. PEARSON. 1961. Kinetics and Mechanism. John Wiley and Sons, Inc., New York.

GLASSTONE, S., K. J. LAIDLER, and H. EYRING. 1941. The Theory of Rate Processes. McGraw-Hill Book Company, New York.

GOLDMAN, D. E. 1943. Potential, impedance, and rectification in membranes. *J. Gen. Physiol.* **27**:37–60.

HECKMANN, K. 1968. Zur Theorie der "Single File"-Diffusion. III. Sigmoide Konzentrationsabhängigkeit unidirektionaler Flüsse bei "Single File"-Diffusion. *Z. Phys. Chem. Neue Folge.* **58**:206–219.

HECKMANN, K. 1972. Single-file diffusion. *In* Biomembranes, Vol. 3, Passive Permeability of Cell Membranes. F. Kreuzer and J. F. G. Slegers, editors. Plenum Press, New York. 127–153.

HECKMANN, K., B. LINDEMANN, and J. S. SCHNAKENBERG. 1972. Current-voltage curves of porous membranes in the presence of pore blocking ions. I. Narrow pores containing no more than one moving ion. *Biophys. J.* **12**:683–702.

HECKMANN, K., and W. VOLLMERHAUS. 1970. Zur Theorie der "Single File"-Diffusion. IV. Vergleich von Leerstellendiffusion und "knock on"-Mechanisms. *Z. Physikal. Chem. Neue Folge.* **71**:320–328.

HECKMANN, K., W. VOLLMERHAUS, J. KUTSCHERA, and E. VOLLMERHAUS. 1969. Mathematische Modelle für reaktionskinetische Phänomene. *Z. Naturforschung Teil B Anorg. Chem. Org. Chem. Biochem. Biophys. Biol.* **24**:664–673.

HILLE, B. 1968. Charges and potentials at the nerve surface: Divalent ions and pH. *J. Gen. Physiol.* **51**:221–236.

HILLE, B. 1970. Ionic channels in nerve membranes. *Prog. Biophys. Mol. Biol.* **21**:1–32.

HILLE, B. 1971. The permeability of the sodium channel to organic cations in myelinated nerve. *J. Gen. Physiol.* **58**:599–619.

HILLE, B. 1972. The permeability of the sodium channel to metal cations in myelinated nerve. *J. Gen. Physiol.* **59**:637–658.

HILLE, B. 1975 *a*. A four-barrier model of the sodium channel. *Biophys. Soc. Annu. Meet. Abstr.* **19**:164a.

HILLE, B. 1975 *b*. Ionic selectivity of Na and K channels of nerve membranes. *In* Membranes—A Series of Advances, Vol. 3, Dynamic Properties of Lipid Bilayers and Biological Membranes. G. Eisenman, editor. Marcel Dekker, Inc., New York. Chap. 4.

HILLE, B. 1975 *c*. An essential ionized acid group in sodium channels. *Fed. Proc.* **34**:1318–1321.

HODGKIN, A. L., and A. F. HUXLEY. 1952 *a*. Currents carried by sodium and potassium ions through the membrane of the giant axon of *Loligo*. *J. Physiol.* (*Lond.*). **166**:449–472.

HODGKIN, A. L., and A. F. HUXLEY. 1952 *b*. The components of membrane conductance in the giant axon of *Loligo*. *J. Physiol.* (*Lond.*). **116**:473–496.

HODGKIN, A. L., and A. F. HUXLEY. 1952 *c*. A quantitative description of membrane current and its application to conduction and excitation in nerve. *J. Physiol.* (*Lond.*). **117**:500–544.

HODGKIN, A. L., A. F. HUXLEY, and B. KATZ. 1952. Measurement of current-voltage relations in the membrane of the giant axon of *Loligo*. *J. Physiol.* (*Lond.*). **116**:424–448.

HODGKIN, A. L., and B. KATZ. 1949. The effect of sodium ions on the electrical activity of the giant axon of the squid. *J. Physiol.* (*Lond.*). **108**:37–77.

HODGKIN, A. L., and R. D. KEYNES. 1955. The potassium permeability of a giant nerve fibre. *J. Physiol.* (*Lond.*). **128**:61–88.

KEYNES, R. D., and E. ROJAS. 1974. Kinetics and steady-state properties of the charged system controlling sodium conductance in the squid giant axon. *J. Physiol.* (*Lond.*). **239**:393–434.

KEYNES, R. D., F. BEZANILLA, E. ROJAS, and R. E. TAYLOR. 1975. The rate of action of tetrodotoxin in the squid giant axon. *Philos. Trans. R. Soc. Lond. B Biol. Sci.* **270**:365–375.

KING, E. L., and C. ALTMAN. 1956. A schematic method of deriving the rate laws for enzyme-catalyzed reactions. *J. Phys. Chem.* **60**:1375–1378.

LÄUGER, P. 1973. Ion transport through pores: A rate-theory analysis. *Biochim. Biophys. Acta.* **311**:423–441.

LEVINSON, S. R., and H. MEVES. 1975. The binding of tritiated tetrodotoxin to squid giant axons. *Philos. Trans. R. Soc. Lond. B Biol. Sci.* **270**:349–352.

MARKIN, V. S., and Y. A. CHIZMADJEV. 1974. Induced Ionic Transport. Nauka, Moscow. (In Russian).

SCHAUF, C. L. 1973. Temperature dependence of the ionic current kinetics of *Myxicola* giant axons. *J. Physiol. (Lond.)*. **235**:197–205.

USSING, H. H. 1949. The distinction by means of tracers between active transport and diffusion. *Acta Physiol. Scand.* **19**:43–56.

WOODBURY, J. W. 1971. Eyring rate theory model of the current-voltage relationship of ion channels in excitable membranes. *In* Chemical Dynamics: Papers in Honor of Henry Eyring. J. Hirschfelder, editor. John Wiley and Sons, Inc., New York.

WOODBURY, J. W., S. H. WHITE, M. C. MACKEY, W. L. HARDY, and D. B. CHANG. 1970. Bioelectrochemistry. *In* Electrochemistry. H. Eyring, W. Jost, and D. Henderson, editors. Academic Press, New York. Chap. 9.

WOODHULL, A. M. 1973. Ionic blockage of sodium channels in nerve. *J. Gen. Physiol.* **61**:687–708.

ZWOLINSKI, B. J., H. EYRING, and C. E. REESE. 1949. Diffusion and membrane permeability. *J. Physiol. Colloid Chem.* **53**:1426–1453.